JACC: BASIC TO TRANSLATIONAL SCIENCE VOL. 8, NO. 10, 2023

ORIGINAL RESEARCH - PRECLINICAL

Loss of Bone Morphogenetic Protein-9 Reduces Survival and Increases MMP Activity After Myocardial Infarction

Shreyas Bhave, PhD, Michele Esposito, MD, Lija Swain, PhD, Xiaoying Qiao, PhD, Gregory Martin, BS, Sakshi Wadhwa, BS, Kay Everett, MD, PhD, Navin K. Kapur, MD

VISUAL ABSTRACT

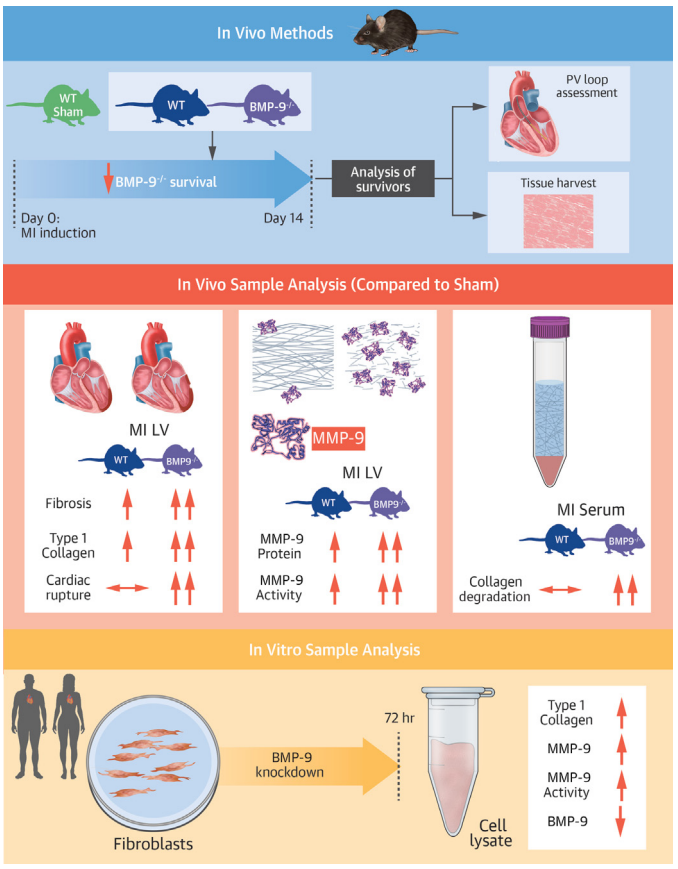

Bhave S, et al. J Am Coll Cardiol Basic Trans Science. 2023;8(10):1318-1330.

HIGHLIGHTS

- **The authors identified a novel function role for BMP-9 in cardiac remodeling after MI.**
- **They report that loss of BMP-9 decreases survival, increases cardiac fibrosis, and increases cardiac rupture after MI.**
- **They observed that loss of BMP-9 increases LV MMP-9 expression and activity and also increases collagen degradation after MI.**

From the Molecular Cardiology Research Institute, Tufts Medical Center, Boston, Massachusetts, USA.
The authors attest they are in compliance with human studies committees and animal welfare regulations of the authors' institutions and Food and Drug Administration guidelines, including patient consent where appropriate. For more information, visit the Author Center.

Manuscript received March 15, 2023; revised manuscript received May 17, 2023, accepted May 17, 2023.

ISSN 2452-302X https://doi.org/10.1016/j.jacbts.2023.05.017

SUMMARY

No studies have explored a functional role for bone morphogenetic protein (BMP)-9, a transforming growth factor-β superfamily ligand, in cardiac remodeling after myocardial infarction (MI). Using BMP-9 null mice, we observed that loss of BMP-9 decreases survival and increases cardiac rupture after MI. We further observed that loss of BMP-9 not only increases collagen abundance, but also promotes matrix metalloproteinase-9 activity and collagen degradation after MI. These findings identify BMP-9 as a necessary component of cardiac remodeling after MI and a potentially important target of therapy to improve outcomes after MI. (J Am Coll Cardiol Basic Trans Science 2023;8:1318–1330) © 2023 Published by Elsevier on behalf of the American College of Cardiology Foundation. This is an open access article under the CC BY-NC-ND license (http://creativecommons.org/licenses/by-nc-nd/4.0/).

ABBREVIATIONS AND ACRONYMS

BMP = bone morphogenetic protein

ECM = extracellular matrix

H-CFb = human cardiac fibroblast

HHT = hereditary hemorrhagic telangiectasia

ICTP = carboxy terminal telopeptide of type 1 collagen

LV = left ventricle/ventricular

MI = myocardial infarction

MMP = matrix metalloproteinase

PINP = amino-terminal propeptide of type 1 collagen

siRNA = small interfering RNA

TGF = transforming growth factor

WT = wild-type

Myocardial infarction (MI) is a major cause of global morbidity and mortality that affects nearly 800,000 patients each year in the United States alone.[1] Cardiac wound healing after MI is a complex and multiphase process that begins with necrosis and apoptosis of cardiomyocytes due to ischemic injury with or without reperfusion followed by the formation of a fibrotic scar.[2] The acute phase of this process involves an inflammatory response and degradation of the extracellular matrix (ECM) followed by collagen synthesis, organization, and deposition within the first few weeks after MI. Cardiac fibrosis is a critical component of this process and a major determinant of cardiac structure and function, which further influences long-term outcomes.[3]

The transforming growth factor (TGF)-β signaling pathway plays a central role in healing by promoting cardiac fibrosis after MI.[4-6] Bone morphogenetic protein-9 (BMP-9) is a member of the TGF-β superfamily of ligands and is implicated in the pathogenesis of the vascular disorder hereditary hemorrhagic telangiectasia (HHT)[7] and pulmonary arterial hypertension.[8,9] Recently, we reported that BMP-9 limits cardiac fibrosis by promoting signaling via the downstream effector Smad1 and reducing the activity of the profibrotic effector Smad3 in murine models of pressure overload induced heart failure.[10] A functional role for BMP-9 in cardiac remodeling after MI remains largely unexplored.

Reorganization of ECM after MI occurs during both early- and late-phase wound healing. In the early phase, matrix metalloproteinase (MMP) activation degrades the ECM followed by a synthetic phase in which collagen synthesis contributes to the generation and deposition of new ECM and cardiac fibrosis.[11] In addition to canonical signaling pathways mediated by TGF-β and BMP-9 as part of scar formation and the wound healing process, recent studies identified that BMP-9 may negatively regulate the expression of MMPs in cancer cell lines.[12,13] MMPs such as MMP-2 and MMP-9 play a critical role in regulating the turnover of ECM in basal and activated states such as during injury.[14,15] We and others reported increased MMP-9 activity in the left ventricle (LV) after MI,[16,17] which is associated with increased mortality in murine models of MI.[18-20] Whether BMP-9 regulates cardiac MMP levels and activity in MI remains unknown.

With this background in mind, we hypothesized that loss of BMP-9 increases MMP activity and collagen turnover which impedes LV scar formation after MI and reduces survival.

METHODS

ANIMALS. All animal experiments were performed in accordance with the Institutional Animal Care and Use Committee protocols. Wild-type (WT) mice were obtained from the Jackson Laboratory. BMP-9$^{-/-}$ mice were generously provided by Dr Se-Jin Lee of John Hopkins University.

MURINE MODEL OF MI. Adult mice 8 to 12 weeks of age were subjected to MI by permanent left coronary artery (LCA) ligation. Briefly, mice were anesthetized under isoflurane inhalation and put on mechanical ventilation using endotracheal intubation. A small incision was made between the ribs to expose the heart. The left coronary artery was located and ligated using a suture to generate an infarct.[21] The wound was closed, and the mice were administered a single dose of buprenorphine SR for postsurgery recovery. Sham mice underwent the exact same process but without the left coronary artery ligation. Mice were observed daily for survival for over 2 weeks.

PRESSURE-VOLUME MEASUREMENTS AND ORGAN HARVESTING. At the end of the study, all mice were subjected to a terminal procedure of pressure-volume measurement using a conductance catheter. For LV

pressure-volume measurements, the carotid artery was located after making a small incision in anesthetized mice. A conductance catheter was inserted into the artery and secured using a suture. Then the catheter was advanced into the LV through the aortic valve. At the end of the recording, mice were euthanized, and tissues were harvested and immediately snap-frozen in liquid nitrogen and stored at −80 °C for further analysis. A section of the LV tissue was also stored in formalin for histology before snap-freezing in liquid nitrogen.

PROTEIN PREPARATION FOR WESTERN BLOT, ZYMOGRAPHY, AND ENZYME-LINKED IMMUNOSORBENT ASSAY. A small piece of snap-frozen tissue was dissected out and homogenized using pestles in T-PER lysis buffer (Thermo Fisher Scientific) supplemented with a protease inhibitor cocktail and phosphatase inhibitor cocktail. The homogenate was incubated on ice for 1 hour and then centrifuged at >13,000 rpm at 4 °C. The supernatant protein extract was separated and used for the preparation of Western blot samples or enzyme-linked immunosorbent assay (ELISA). For the zymography assay, a protease inhibitor cocktail was excluded from the lysis buffer. For protein extraction from cells, the same buffer was used to lyse the cells, followed by centrifugation to separate the protein extracts.

Western blot. Protein samples were prepared using an equal amount of protein and were denatured by heating at 100 °C in Laemmli buffer (Boston Bioproducts). Proteins were then separated on a mini PROTEAN TGX 4-15% gel (Bio-Rad) and transferred onto the PVDF membrane (MilliporeSigma). The membrane was blocked using a 5% solution of dry milk in phosphate-buffered saline with Tween 20 for 1 hour. For detection of specific proteins, membranes were incubated in specific antibodies overnight. The next day, the membranes were washed 3 times for 10 minutes each with a 5% solution of dry milk in phosphate-buffered saline with Tween 20. Membranes were then incubated with appropriate horseradish peroxidase-conjugated secondary antibody for 1 hour at room temperature. At the end, membranes were washed 3 times with phosphate-buffered saline with Tween 20 for 10 minutes each. Protein bands were visualized using Pierce ECL Western Blotting Substrate (Thermo Fisher Scientific) on a FluorChem E FE0504 imaging machine (ProteinSimple). ImageJ 1.52a (National Institutes of Health) was used to quantify the band density. The following primary antibodies were used for the analysis: pSMAD1/5 (9516; Cell Signaling Technology), SMAD1 (9743; Cell Signaling Technology), SMAD3 (9513; Cell Signaling Technology), pSMAD3 (9520; Cell Signaling Technology), pSMAD2 (3108; Cell Signaling Technology), SMAD2 (5339; Cell Signaling Technology), type 1 collagen (ab88147; Abcam), α-smooth muscle actin (α-SMA) (ab5694; Abcam), troponin T (ab8295; Abcam), periostin (ab14041; Abcam), BMP-9 (MAB3209; R&D Systems), endoglin (AF1320; R&D Systems), MMP-9 (AF909; R&D Systems), MMP2 (AF1488; R&D Systems), Flt-1 (Fms related receptor tyrosine kinase 1) (AF471; R&D Systems), vascular endothelial growth factor (VEGF) (NB100-664; Novus), CD-31 (NB 100-2284; Novus), and GAPDH (MAB374; MilliporeSigma).

Zymography. To assess the MMP enzymatic activity within infarcted and noninfarcted zones, infarcted myocardium was carefully isolated for protein extraction. Rest of the LV was used as noninfarcted zone. Fresh protein samples were prepared using sample buffer and immediately separated on gels containing 10% gelatin. At the end of the separation, gels were carefully incubated in renaturation buffer for 30 minutes at room temperature. The buffer was discarded and gels were incubated in developing buffer for 1 hour with gentle shaking. The developing buffer was replaced with fresh developing buffer and gels were placed in an incubator at 37 °C. The next morning, buffer was removed and gels were incubated in the SimplyBlue SafeStain (Thermo Fisher Scientific) for 4 hours at room temperature with shaking. At the end, gels were washed in Milli Q water (MilliporeSigma) to remove excess stain and digestion bands were visualized on a FluorChem E FE0504 imaging machine (ProteinSimple) machine. Bands were quantified using ImageJ software.

Enzyme-linked immunosorbent assay. Serum samples were diluted and analyzed using the manufacturer's (MyBiosource) protocol to measure the carboxy-terminal telopeptide of type 1 collagen (ICTP) (MBS2701081) and amino-terminal propeptide of type 1 collagen (PINP) (MBS2702748) levels. The manufacturer's (R&D Systems) protocol was followed for the measurements of TGF-β1 (DB100B) and BMP-9 (DY5566) in LV tissue lysates. The TGF-β enzyme-linked immunosorbent assay measured both active and inactive TGF-β. LV tissue levels of inflammatory markers were measured using enzyme-linked immunosorbent assay as per the manufacturer's protocol for interleukin-6 (MBS9360517; MyBiosource), tumor necrosis factor α (MBS043098; MyBiosource) and neutrophil gelatinase-associated lipocalin (MLCN20; R&D Systems).

HISTOLOGY. Formalin-fixed samples were embedded in paraffin and subsequently sectioned. Sections were

then mounted onto the slides and deparaffinized by heating in an oven at 60 °C, followed by 3 exchanges of HistoChoice (Sigma-Aldrich); 2 exchanges of 100% ethanol; 1 exchange in each of 95% ethanol, 70% ethanol, and 50% ethanol; and finally into Milli Q water. Picrosirius red staining (ab245887; Abcam) was performed using the manufacturer's protocol.

CELL CULTURE. The Tufts Medical Center Institutional Review Board approved the collection of human tissue for cell culture. Human cardiac fibroblasts (H-CFbs) were isolated from myocardial tissue harvested during cardiac surgery at Tufts Medical Center, then cultured in FBM Basal Medium supplemented with insulin, fibroblast growth factor, Gentamicin sulfate, and fetal bovine serum (Lonza). Cells were starved in serum-free media for 24 hours before transfection. Oligofectamine-siRNA (Thermo Fisher Scientific) mixture was then added onto the cells. After 6 hours of incubation at 37 °C and 5% CO_2, serum-supplemented media was added and cells were cultured for another 48 hours. At the end of 48 hours, cells were harvested for RNA and protein extraction.

STATISTICAL ANALYSIS. In all graphs and the table data are presented as mean ± SD. The Shapiro-Wilk test was used to confirm the normal distribution of dataset. For comparison among the groups, Student's *t* test was used in case of comparison between 2 groups. For comparing more than 2 groups, analysis of variance was used followed by Tukey's post hoc honest significant difference test for multiple pairwise comparisons. For survival analysis, Kaplan-Meier curves were plotted and compared with the log-rank test. All statistical analysis was done using GraphPad Prism 9.3.1 (GraphPad Software). A P value of <0.05 was considered statistically significant.

RESULTS

LOSS OF BMP-9 DECREASES SURVIVAL AFTER MI AND IS ASSOCIATED WITH CARDIAC RUPTURE. To understand the role of BMP-9 after MI, WT and BMP-$9^{-/-}$ mice were subjected to left coronary artery ligation for 14 days. BMP-$9^{-/-}$ mice demonstrated significantly reduced survival after MI as compared with WT mice (**Figure 1A**), with all deaths occurring within 7 days of left coronary artery ligation in both groups. Subsequent necropsy analysis revealed that 86% (n = 6 of 7) of deaths in the BMP-$9^{-/-}$ group were associated with transmural myocardial rupture compared with zero ruptures in WT mice (**Figures 1A and 1B**). Compared with WT, levels of BMP-9 were nearly undetectable in BMP-$9^{-/-}$ mice by immunoblot analysis, real-time polymerase chain reaction, and enzyme-linked immunosorbent assay (**Figures 1C-1E**). Picrosirius staining confirmed a >5-fold increase in LV fibrotic area in BMP-$9^{-/-}$ mice compared with WT mice after MI ($P = 0.001$) (**Figures 1F and 1G**).

To support cellular contributions to the observed phenotypes related to BMP-9 function in the heart, we quantified BMP-9 levels in isolated murine cardiac myocytes, endothelial cells, and cardiac fibroblasts. BMP-9 expression was observed in both fibroblasts and endothelial cells but in not cardiac myocytes (Supplemental Figure 1A). Both WT and BMP-$9^{-/-}$ mice exhibited significantly reduced LV ejection fraction and stroke work compared with sham mice after MI. Compared with WT sham mice, both LV end-systolic ($P = 0.012$) and LV end-diastolic ($P = 0.011$) volumes were significantly increased in BMP-$9^{-/-}$ mice but not in WT mice after MI (**Table 1**). These observations suggest that loss of BMP-9 decreases survival, increases LV fibrosis and myocardial rupture, and further promotes maladaptive cardiac remodeling after MI.

BMP-$9^{-/-}$ MICE HAVE INCREASED FIBROSIS AFTER MI. Next, we examined the effect of BMP-9 loss on TGF-β1 levels and canonical Smad signaling. Loss of BMP-9 significantly increased messenger RNA and protein levels of TGFb1 in the LV ($P = 0.013$ for messenger RNA and $P = 0.026$ for protein measured by ELISA) (**Figures 2A and 2B**). We further observed that loss of BMP-9 significantly increased LV levels of type 1 collagen, the profibrotic TGF-β co-receptor endoglin, and α-smooth muscle actin protein compared with WT MI mice (**Figures 2C to 2E**). Loss of BMP-9 reduced levels of phosphorylated Smad1/5 by 80% ($P = 0.025$) and increased levels of phosphorylated Smad3 and Smad2 by 7-fold and 4-fold, respectively, compared with WT mice after MI (**Figures 2F to 2H**). Compared with WT, loss of BMP-9 significantly increased LV protein levels of vascular endothelial growth factor and the type 1 vascular endothelial growth factor receptor FLT-1 compared with WT sham (Supplemental Figure 1B). These finding suggest that loss of BMP-9 promotes profibrotic signaling via Smad3 and endoglin and may promote proangiogenic signaling in the LV after MI.

LOSS OF BMP-9 PROMOTES MMP-9 EXPRESSION AND ACTIVITY IN VIVO AFTER MI. To explore the mechanisms underlying the increased incidence of cardiac rupture in BMP-$9^{-/-}$ mice despite increased collagen abundance and LV fibrosis after MI, we measured expression and activity of MMPs. Loss of BMP-9 increased LV MMP-9 protein levels in BMP-$9^{-/-}$ mice ($P < 0.01$) compared with WT mice after MI (**Figure 3A**). MMP2 protein levels were not

FIGURE 1 BMP-9 Loss Leads to Decreased Survival and Increased Incidence of Cardiac Rupture and Fibrosis

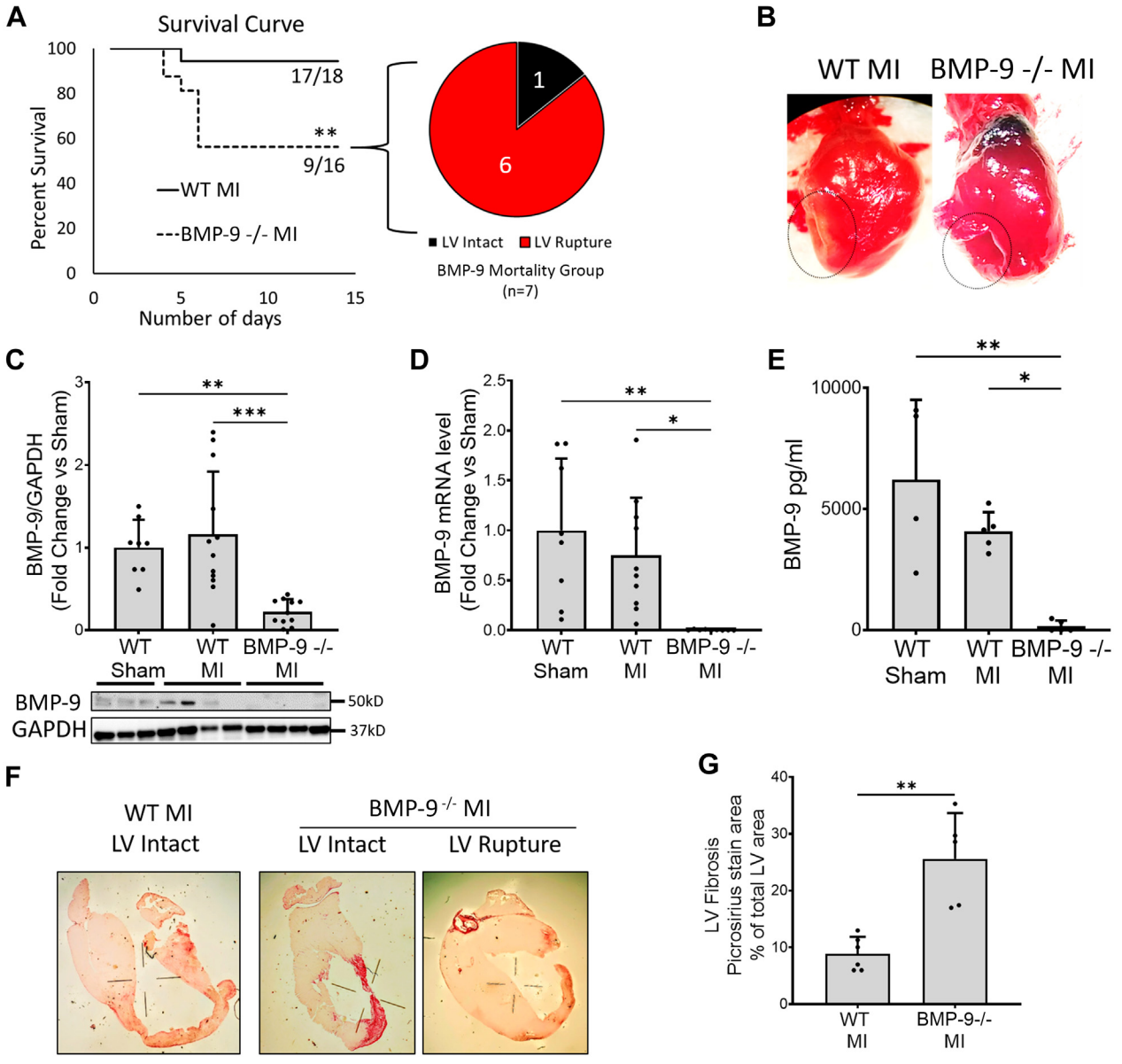

Wild-type (WT) or BMP-9$^{-/-}$ mice were subjected to left anterior descending artery ligation to induce myocardial infarction (MI) and were allowed to recover over 14 days to assess their survival. (A) Survival plot showing the percentage of mice survived over 14 days after MI and incidences of cardiac ruptures among BMP-9$^{-/-}$ deaths. * $P < 0.05$, log-rank test, n = 16 to 18. (B) Images showing MI with intact myocardium (WT MI) and ruptured myocardium (BMP-9$^{-/-}$) observed at necropsy after MI. (C) Relative bone morphogenic protein-9 (BMP-9) protein levels in the left ventricle (LV) of mice from indicated groups corrected for GAPDH protein levels. (D) Fold change in BMP-9 messenger RNA (mRNA) levels in LV tissues corrected for 18s rRNA expression in indicated groups. (E) BMP-9 protein levels in LV tissue lysates detected by enzyme-linked immunosorbent assay in indicated groups. *$P < 0.05$, ***$P < 0.001$, 1-way analysis of variance followed by Tukey's honest significant difference, n = 5 to 7. (F, G) Picrosirius staining of an infarcted LV cross-section showing the extent of fibrosis along with a graph of quantification of the fibrotic area as percentage of total LV area. *$P < 0.05$ Student's *t* test, n = 5.

significantly increased in the LV after MI in both WT and BMP-9$^{-/-}$ mice compared with WT sham (Figure 3C). MMP-9 and MMP2 enzymatic activity were significantly higher within the infarct zone compared with noninfarct zones in both WT and BMP-9$^{-/-}$ mice (Figures 3B and 3D). MMP-9 activity within the infarct zone was significantly higher in BMP-9$^{-/-}$ mice compared with WT mice (Figure 3B). No significant difference in MMP2 activity was observed between WT and BMP-9$^{-/-}$ infarct zones.

To explore the time course of changes in MMP-9 expression and activity after MI, WT and BMP-9$^{-/-}$ mice were subjected to 1 week of left coronary ligation. No deaths were observed in WT mice (n = 5). In contrast, 57% (n = 4 of 7) of BMP-9$^{-/-}$ mice died within 1 week. Compared with WT MI, LV type I collagen protein levels increased 1 week after MI in BMP-9$^{-/-}$ mice. Levels of phosphorylated Smad2 and Smad3 increased in BMP-9$^{-/-}$ mice 1 week compared with WT mice after MI. Phosphorylated Smad1 levels were nonsignificantly decreased in BMP-9$^{-/-}$ mice after 1 week compared with WT mice after MI. LV α-smooth muscle actin and MMP-9 protein levels increased in both WT and BMP-9$^{-/-}$ mice, but MMP-9 activity levels were increased only in BMP-9$^{-/-}$ mice. These data suggest that compared with WT mice, loss of BMP-9 increases MMP-9 activity beginning within 1 week after MI (Supplemental Figure 2).

TABLE 1 Hemodynamic Assessment 2 Weeks After MI

	WT Sham	WT MI	BMP-9$^{-/-}$ MI
Body weight, g	28.28 ± 1.08	26.79 ± 1.6	26.75 ± 6.01
Tibia length, mm	17.46 ± 0.21	17.40 ± 0.16	17.34 ± 1.46
LV weight/tibia length, g/mm	6.58 ± 0.80	7.62 ± 1.08	7.46 ± 0.82
Lung weight/tibia length, g/mm	9.91 ± 2.25	9.92 ± 1.44	8.99 ± 2.02
EDV, μL	47.44 ± 12.23	60.88 ± 13.44	75.25 ± 14.60[a]
EDP, mm Hg	4.75 ± 5.26	7.00 ± 5.01	4.60 ± 5.16
ESV, μL	40.10 ± 10.74	51.88 ± 10.30	61.00 ± 9.64[a]
ESP, mm Hg	88.42 ± 16.10	75.44 ± 8.90	82.40 ± 12.15
EF, %	37.72 ± 5.54	24.77 ± 4.82[b]	21.25 ± 6.17[b]
Stroke work	1,516.70 ± 422.12	860.56 ± 242.40[b]	768.75 ± 135.21[b]

Values are mean ± SD. The table shows pressure-volume measurements and organ weight assessment. Data were analyzed by analysis of variance followed by Tukey's post hoc honest significant difference test for multiple pairwise comparisons. [a]$P < 0.05$ vs WT sham. [b]$P < 0.01$ vs WT sham.

EDP = end-diastolic pressure; EDV = end-diastolic volume; EF = ejection fraction; ESP = end-systolic pressure; ESV = end-systolic volume; LV = left ventricular; MI = myocardial infarction; WT = wild-type.

To assess the effect of BMP-9 loss on cardiac inflammatory responses after MI, we quantified LV levels of Interleukin-6, tumor necrosis factor a, and neutrophil gelatinase-associated lipocalin in WT and BMP-9$^{-/-}$ mice after both 1 and 2 weeks after MI. Interleukin 6 levels were significantly increased 2 weeks after MI in WT mice but not in BMP-9$^{-/-}$ mice. Neutrophil gelatinase-associated lipocalin levels were increased in BMP-9$^{-/-}$ mice 1 week after

FIGURE 2 Loss of BMP-9 Increased Profibrotic Signaling, Collagen, and Endoglin Levels in the LV 2 Weeks After MI

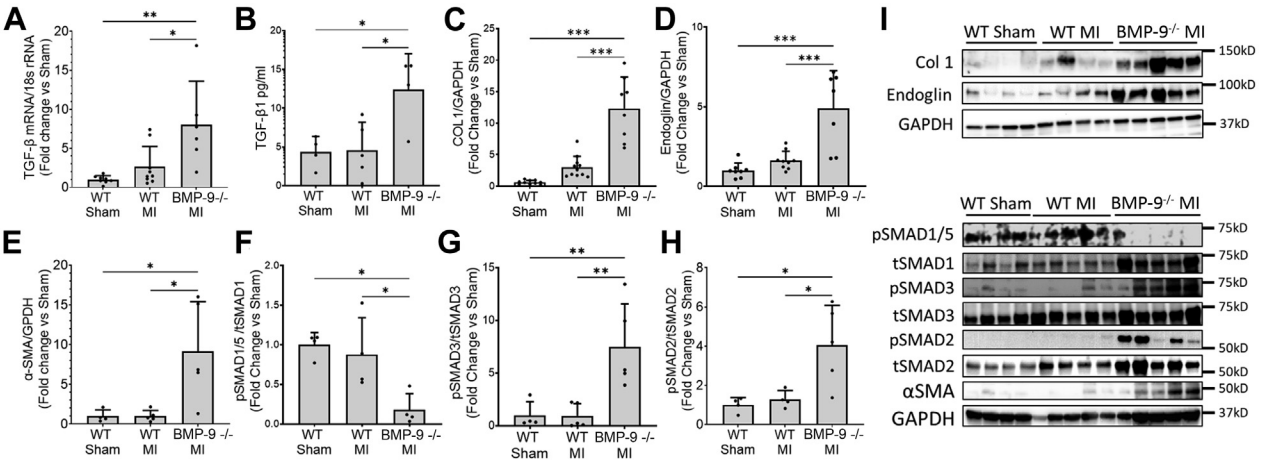

(A) Transforming growth factor β1 (TGF-β1) messenger RNA levels measured by real-time quantitative polymerase chain reaction and (B) TGF-β1 protein levels measured by enzyme-linked immunosorbent assay in LVs of indicated groups. Western blot images and corresponding quantification graphs for relative protein expression of (C) type 1 collagen, (D) endoglin, and (E) α-smooth muscle actin (α-SMA) corrected for GAPDH protein levels. Relative protein levels of (F) pSMAD1/5, (H) pSMAD3, and (H) pSMAD2 corrected for corresponding total SMADs. *$P < 0.05$, **$P < 0.01$, ***$P < 0.001$, 1-way analysis of variance followed by Tukey's honest significant difference, n = 5 to 10. rRNA = ribosomal RNA; abbreviations as in Figure 1.

FIGURE 3 BMP-9$^{-/-}$ Mice Have Increased Levels of MMP-9 Protein and Enzymatic Activity 2 Weeks After MI

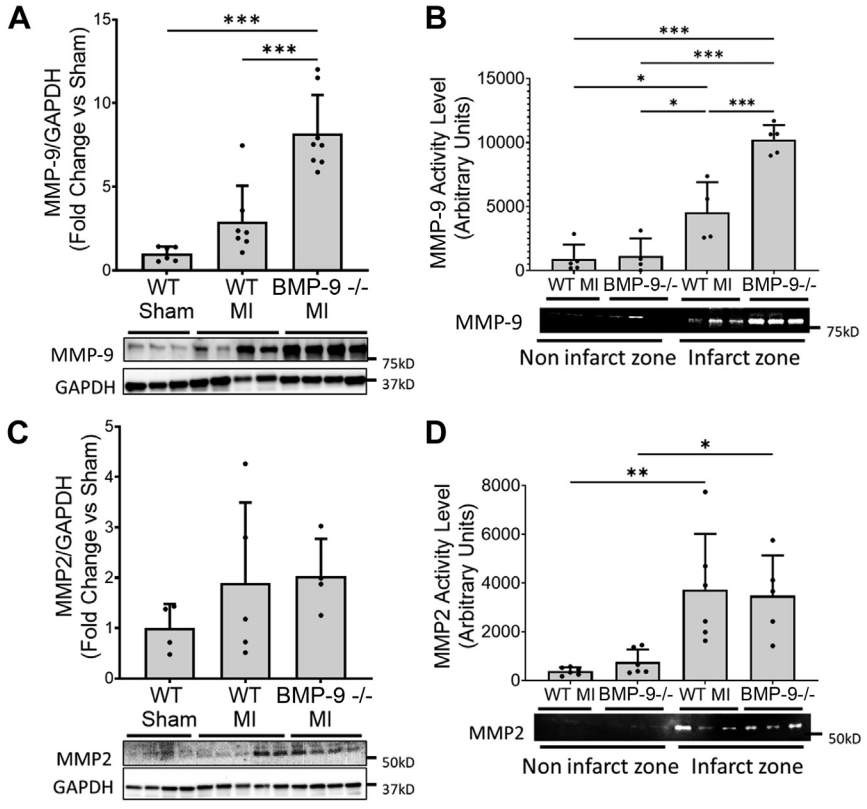

Immunoblots, zymographs, and corresponding quantification graphs for (A) Western blot images showing relative matrix metalloproteinase-9 (MMP-9) protein levels corrected for GAPDH protein levels and (B) zymography gel image and corresponding quantification showing relative MMP-9 enzyme activity levels in infarcted and noninfarcted regions of LVs of mice from indicated groups 2 weeks after MI. (C) Western blot images showing relative MMP2 protein levels corrected for GAPDH protein levels in LVs of indicated groups and (D) zymography gel image and corresponding quantification showing relative MMP2 enzyme activity levels in infarcted and noninfarcted regions of LVs of mice from indicated groups 2 weeks after MI. *$P < 0.05$, **$P < 0.01$ ***$P < 0.001$, 1-way analysis of variance followed by Tukey's honest significant difference, n = 5 to 7. Abbreviations as in Figure 1.

MI but not 2 weeks after MI and not in WT mice after MI. Tumor necrosis factor a levels were unchanged across all groups (Supplemental Figure 3).

LOSS OF BMP-9 INCREASES CIRCULATING MARKERS OF COLLAGEN DEGRADATION AFTER MI. To test whether increased MMP-9 levels promote collagen degradation, we quantified biomarkers of type 1 collagen synthesis and degradation. Serum levels of PINP, a marker of type 1 collagen synthesis, were unchanged (Figure 4A) between WT and BMP-9$^{-/-}$ mice after MI. In contrast, compared with WT, loss of BMP-9 increased circulating levels of ICTP, a marker of type I collagen degradation, by 3-fold ($P = 0.019$) (Figure 4B). The circulating ratio of ICTP/PINP was significantly higher in BMP-9$^{-/-}$ mice ($P = 0.022$) compared with WT mice after MI (Figure 4C), suggesting increased collagen degradation in the absence of BMP-9.

LOSS OF BMP-9 PROMOTES MMP-9 EXPRESSION AND ACTIVITY IN H-CFbs. To further assess whether BMP-9 limits MMP-9 expression and activity, we silenced BMP-9 in H-CFbs and confirmed efficient knockdown with reduced messenger RNA levels of both BMP-9 and its downstream target, ID1 (inhibitor of DNA binding 1), and further confirmed reduced protein levels of BMP-9 (Figures 5A, 5B, and 5J). Silencing BMP-9 increased type 1 collagen and both MMP-9 protein and activity levels compared with cells treated with a scrambled small interfering RNA (siRNA) (Figures 5C to 5E and 5J). Loss of BMP-9 increased levels of phosphorylated Smad3, endoglin, and α-smooth muscle actin without affecting levels of

FIGURE 4 Loss of BMP-9 Is Associated With Increased Levels of Type 1 Collagen Degradation Marker

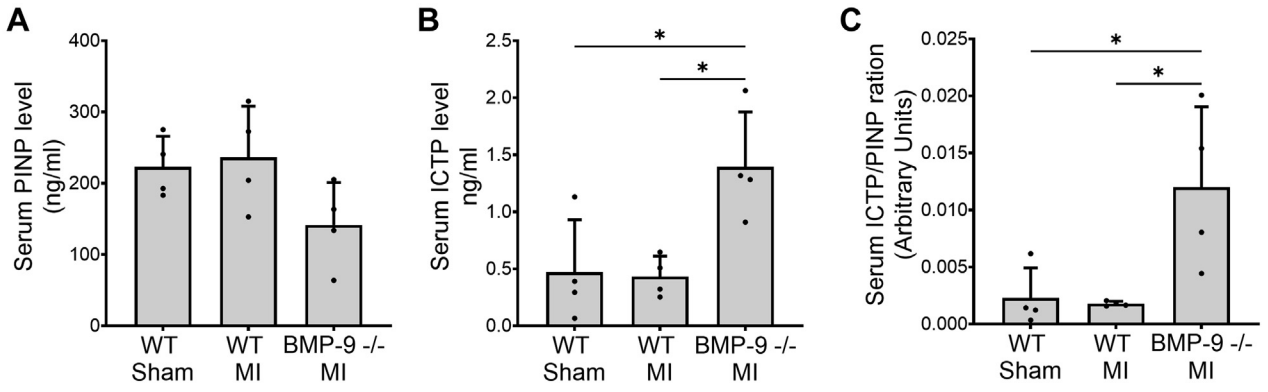

Serum levels of (A) procollagen type I N-terminal propeptide (PINP) and (B) type 1 collagen C-terminal telopeptide (ICTP) 2 weeks after MI. (C) Bar graph showing increased serum ICTP/PINP ratio in BMP-9$^{-/-}$ mice 2 weeks after MI indicating increased type 1 collagen degradation. *$P < 0.05$, 1-way analysis of variance followed by Tukey's honest significant difference, n = 4 to 5. Abbreviations as in Figure 1.

phosphorylated Smad1 (Figures 5F to 5J). These data support that loss of BMP-9 promotes MMP-9 expression, collagen production, and activation of cardiac fibroblasts.

DISCUSSION

We report a novel functional role for BMP-9 as a critical mediator of cardiac remodeling after MI. First, using BMP-9 null mice, we observed that loss of BMP-9 is associated with reduced survival after MI. Second, despite a significant increase in LV collagen abundance in BMP-9 null mice, we observed a significantly higher rate of cardiac rupture and LV dilatation compared with WT control animals. We further observed that consistent with reduced BMP-9 activity, fibroblast activation and profibrotic signaling via Smad3 and endoglin increased while signaling via Smad1 decreased in the LV after MI. Third, loss of BMP-9 increased MMP-9 levels and activity in the LV and was associated with increased circulating markers of collagen degradation. Finally, to further establish an interaction between BMP-9 and MMP-9, we silenced BMP-9 in H-CFbs and observed increased MMP-9 levels and activity as well as signaling via Smad3 and endoglin. Collectively, these data identify BMP-9 as a novel master regulator of collagen turnover and MMP-9 activity in the LV and further suggest that BMP-9 may be an important target of therapy to improve survival and limit maladaptive cardiac remodeling after MI.

Fibrosis plays a critical role post-MI cardiac remodeling. Prior reports have illustrated that the TGF-β-BMP-9 pathway regulates collagen deposition in pressure overload-mediated heart failure in murine models.[4,10] We recently reported that BMP-9 signaling via Smad1 opposes fibrosis and loss of BMP-9 is associated with impaired cardiac function and increased fibrosis in murine models of heart failure.[10] However, a functional role for BMP-9 in cardiac remodeling after MI has not been explored. In this study, we report a novel role of BMP-9 in cardiac remodeling after MI. We identified that loss of BMP-9 reduces survival after MI and promotes myocardial rupture. Due to advances in coronary reperfusion and systems of care for MI, myocardial rupture after MI is uncommon but remains a life-threatening condition. The incidence of cardiac rupture is more frequent in murine models of LAD ligation and provides us with a phenotype to study the mechanisms of myocardial wound healing after MI. We observed cardiac rupture among the BMP-9$^{-/-}$ mice within the first 7 days after MI. Prior reports have observed LV rupture within 2 to 8 days after MI irrespective of strain and genotype[18,19,22]; however, in our studies we did not observe any rupture phenotype among WT mice. One explanation could be due to variability of infarct size in preclinical models of MI; however, in our study, left coronary ligation was performed consistently across all studies by the same blinded operator.

After MI, a balance in profibrotic Smad3 signaling and antifibrotic Smad1 signaling is critical for physiological recovery.[6] Imbalance in these 2 signaling pathways with increased Smad3 activity results in excessive collagen deposition, cardiac fibrosis, and poor physiological outcomes. In our model, consistent with previous findings, we observe that loss of

FIGURE 5 siRNA-Mediated Knockdown of BMP-9 Leads to Increased MMP-9 Protein Expression and Enzymatic Activity in H-CFbs

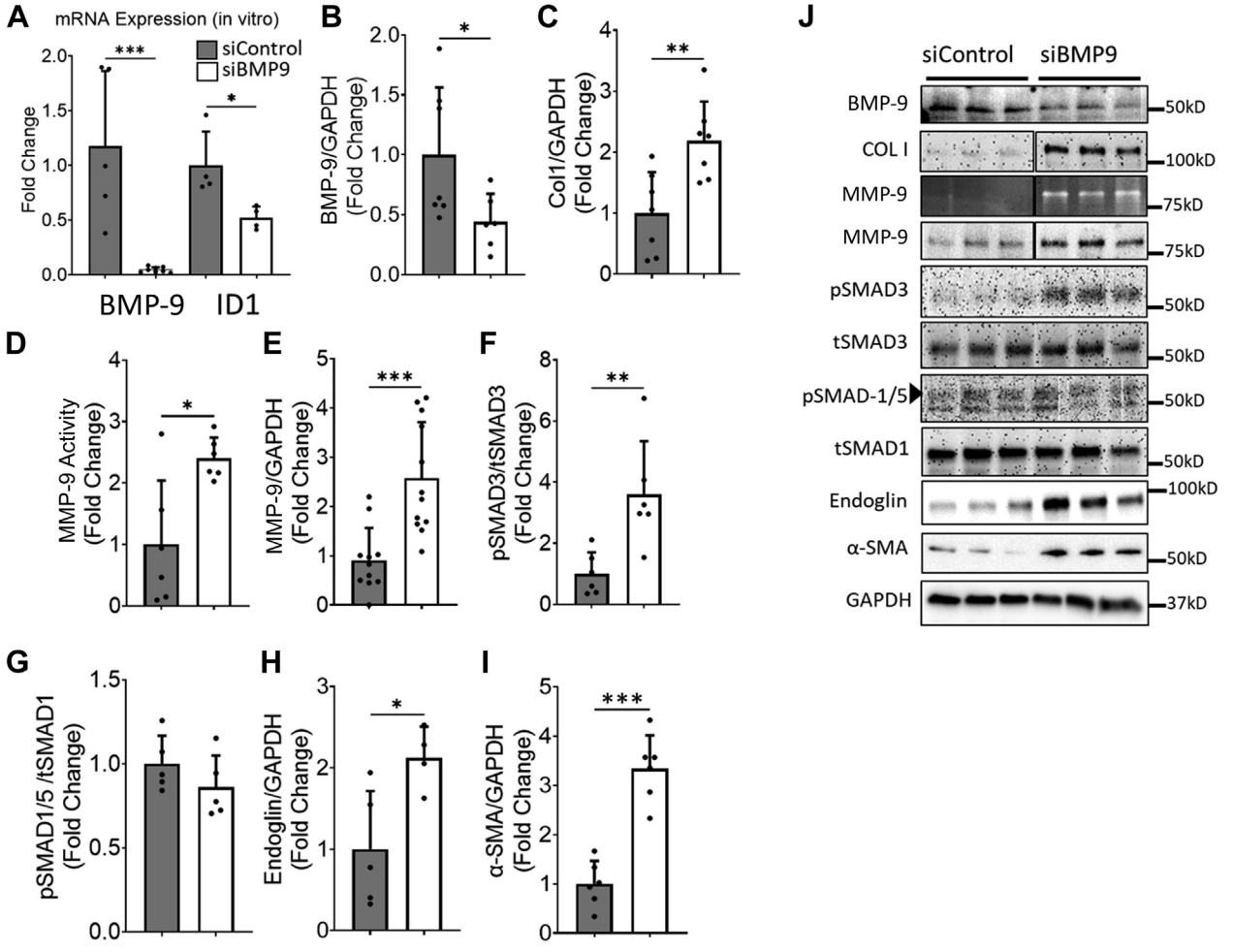

(A) Bar graph showing fold changes in BMP-9 and ID1 (inhibitor of DNA binding 1) Messenger RNA expression levels in human cardiac fibroblasts (H-CFbs) transfected with control (siControl) or BMP-9 small interfering RNA (siBMP-9). (B) Graphs showing relative protein expression of BMP-9 C type 1 collagen. (D) Graph showing relative MMP-9 activity assessed by zymography. Graphs showing relative protein expression of (E) MMP-9, (F) pSMAD3 corrected for tSMAD3, (G) pSMAD1/5 corrected for tSMAD1, (H) endoglin, and (I) α-smooth muscle actin in H-CFbs transfected with scrambled siRNA (siControl) or siRNA against BMP-9. (J) Corresponding zymography gel image and Western blot images. *$P < 0.05$, **$P < 0.01$ ***$P < 0.001$. Student's t test, n = 4 to 6. Abbreviations as in Figures 1 to 3.

BMP-9 tips the balance toward profibrotic Smad3 signaling with attenuation of Smad1 phosphorylation. This is also associated with increased TGF-β levels. Whether loss of BMP-9 increases TGF-β levels or loss of Smad1 signaling and worsening cardiac function further increases TGF-β levels requires further investigation.

During the first few days after MI, collagen synthesis and deposition are balanced by profibrotic signaling pathways and MMP activity. If collagen production persists without degradation, excessive fibrosis increases scar burden and thereby impairs cardiac function and creates the substrate for ventricular arrhythmias.[23] We recently observed that loss of BMP-9 increases cardiac fibrosis in LV pressure overload models[9] and therefore anticipated that BMP-9 null mice may have more stable scar formation and be protected from death and cardiac rupture after MI. Interestingly, we observed significantly more fibrosis and collagen deposition in BMP-9 null mice that were associated with lower survival and a significantly higher incidence of cardiac rupture. This suggested that while these mice may have more abundant myocardial collagen content and cardiac fibrosis, the quality of the scar may be poor and susceptible to rupture.

The majority of prior reports exploring myocardial integrity and cardiac rupture in murine models of MI strongly suggested a potential role for increased expression and activity of MMPs as a potential reason for poor scar integrity.[18,19] Furthermore, studies have shown that inhibition of MMPs can reduce the incidence of cardiac rupture in murine models.[20,24,25] This prompted us to investigate the MMP activities and levels in MI. Indeed, we found that BMP-9$^{-/-}$ mice had increased expression of MMP-9 and increased activity of both MMP-9 and MMP2 in the LV after MI. MMP2 and MMP-9 have strong collagenase activity and regulate dynamic changes in the ECM.[26] Interestingly, many cancer cells utilize increased MMPs activity to alter the ECM and invade tissues.[27,28] The TGF-β-BMP-9 pathway has also been shown to regulate MMP activity and level in various cancer cell models.[27,29,30] The role of the TGF-β-BMP-9 pathway in MMP regulation is not known. We investigated whether BMP-9 has direct control over the expression and activity of MMPs in cardiac fibroblasts. Indeed, our in vitro data show that siRNA-mediated loss of BMP-9 leads to increased expression and activity of MMP-9. These findings are consistent with our in vivo data, and for the first time, we show a direct link between BMP-9 and MMP-9 in the heart. These findings are significant as this adds a point of intersection between cancer therapies and management of myocardial wound healing after MI. Furthermore, this also signifies the importance of a cellular process that can be targeted for cancer treatment and may have an impact on critical organs such as the heart. Interestingly, currently, the TGF-β pathway is under intense investigation for developing novel therapies for both cancers and cardiovascular diseases. Recently an antibody-based molecule that targets BMP receptors entered the third phase of clinical trials for treatment of pulmonary arterial hypertension (NCT03496207).[31,32] How this drug affects cardiac remodeling after MI is yet to be determined.

Findings of this study may be important for patients with HHT. There are limited comprehensive reports that have studied the cardiac remodeling after MI in the HHT population. Most of these studies are limited to case reports. TGF-β signaling pathway plays central role in the development of HHT. Mutations in proteins involved in this pathway are associated with different types of HHTs. Mutations in endoglin (type 1), ALK1 (type 2), and SMAD4 (juvenile polyps HHT) are associated with formation of arteriovenous malformations—a classic symptom of HHT. Although these type differ slightly, they all share common phenotype of bleeding. A more recent type of HHT, type 5, has been associated with mutations in BMP-9,[7] which leads to altered BMP-9 protein processing, which is associated with skin lesions and nosebleeds. Interestingly, we did not observe any subcutaneous as well as internal bleeding in our BMP-9$^{-/-}$ mouse model, which is consistent with previous observation.[10] In contrast to this, conditional deletion of the ALK1 gene leads to gastrointestinal bleeding similar to the HHT phenotype.[33] This suggests that while the BMP-9-ALK1 pathway is important in the development of HHT, the loss of BMP-9 and ALK1 differentially affect the vascular remodeling. While HHT patients have an increased risk of thrombotic events due to frequent incidences of bleeding and hemorrhage, how their genetic predisposition affects the cardiac recovery after MI remains unknown.[34-36]

Finally, to explore whether increased MMP activity increases collagen degradation, we assessed the biomarkers for collagen degradation. Indeed, our data indicated that BMP-9$^{-/-}$ mice, which have significantly higher levels and activity of MMPs, have elevated levels of biomarkers associated with collagen degradation. PINP of acts as a biomarker for type I collagen synthesis, while ICTP serves as a surrogate for its degradation.[37] The relative levels of these biomarkers indicate the overall turnover of collagen. These findings raise an important question about the quality vs quantity of collagen. While BMP-9$^{-/-}$ mice have increased fibrosis and collagen deposition, they also have increased mortality due to cardiac rupture. Our results suggest that the quality of collagen is critical to stabilize the scar and prevent the rupture after MI, as degradation of collagen in BMP-9$^{-/-}$ mice is associated with significantly lower survival despite having increased fibrosis. Furthermore, most of the MMP-9 activity is concentrated in the infarct region of the heart (**Figure 3**), which is a major site of fibrosis due to collagen deposition (**Figure 1F**). Previous reports have indicated that after MI, collagen fibers have weaker structural integrity due to lower crosslinking and overall organization.[38] Whether loss of BMP-9 plays a role in collagen crosslinking and its organization remains unknown. Future studies are required to confirm the effect of BMP-9 loss of matrix spatial organization and fiber structure. **Figure 6** illustrates our finding, in which intact BMP-9 activity after MI leads to a physiological process that results in the stabilization of cardiac wound through

FIGURE 6 BMP-9 Is Required for Survival After MI and Its Loss Is Associated With Increased Incidences of Myocardial Rupture and Death

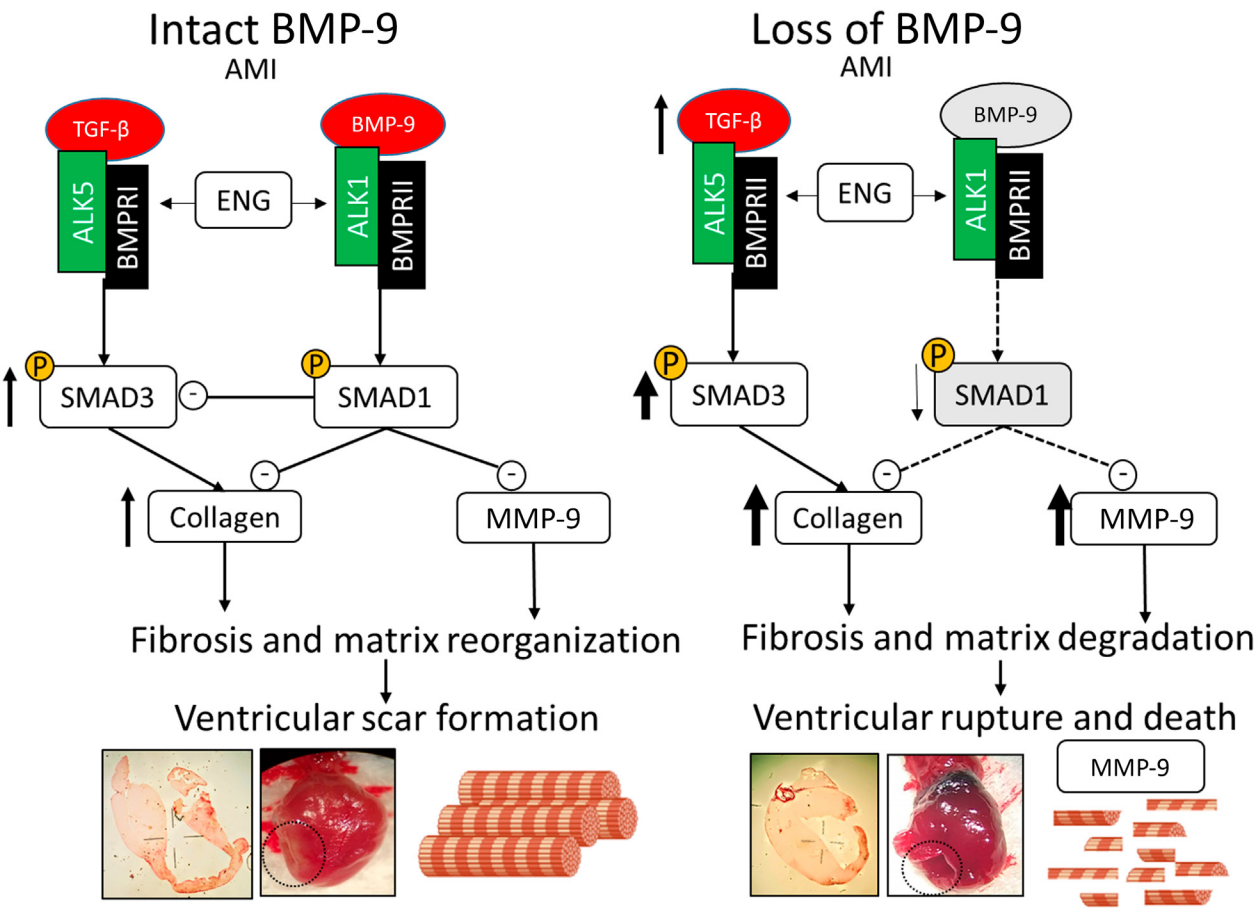

Central figure depicting the mechanism of the TGF-β/BMP-9-mediated wound healing process after MI. The intact BMP-9 axis preserves physiological scar formation while, loss of BMP-9-medicated signaling increases fibrosis and myocardial rupture along with collagen degradation. AMI = acute myocardial infarction; other abbreviations as in Figures 1 to 3.

scar formation. The loss of the BMP-9 axis leads to increased SMAD3 mediated activity and increased fibrosis, but the loss of SMAD1 activity is associated with collagen degradation and reduced survival after MI due to increased incidences of ventricular rupture.

STUDY LIMITATIONS. First, we have used a whole-body BMP-9 knockout mouse model. Future studies are required to establish a cell-specific effect of BMP-9 in cardiac remodeling. Second, we performed studies in male mice only. Interestingly, a previous report has shown that female mice are protected from cardiac rupture irrespective of strain.[39] How sex hormones affect myocardial recovery and survival after MI needs further investigation. Third, we employed a model of left coronary artery ligation as opposed to ischemia-reperfusion injury to limit variability in LV injury associated with MI. The physiological assessment by pressure-volume loop analysis was done on surviving mice at the end of 2 weeks after MI. This created bias in the data collection, as physiological data of dead mice were not collected and included in the final analysis. Finally, we have used C57BL6 mice as WT control animals that have same genetic background

as BMP-9$^{-/-}$ mice. Due to low litter size and litter numbers associated with BMP-9$^{-/-}$ breeding, littermates were not used.

CONCLUSIONS

We report a novel functional role for BMP-9 in cardiac remodeling after MI. Based on recent observations showing that BMP-9 may be a critical regulator of cardiac fibrosis, our findings provide new mechanistic insight by illustrating that BMP-9 is necessary for survival and that loss of BMP-9 is associated with an increase in cardiac rupture, which occurs despite increased collagen abundance and may be driven by higher levels of MMP-9 activity and collagen degradation in the absence of BMP-9. These findings identify BMP-9 as a potentially important target of therapy to improve outcomes for millions of individuals experiencing MI.

FUNDING SUPPORT AND AUTHOR DISCLOSURES

This work was supported by National Heart, Lung, and Blood Institute grants R01HL133215-05 and R01HL139785-01. The authors have reported that they have no relationships relevant to the contents of this paper to disclose.

ADDRESS FOR CORRESPONDENCE: Dr Navin K. Kapur, Molecular Cardiology Research Institute, Tufts Medical Center, 800 Washington Street, Box #80, Boston, Massachusetts 02111, USA. E-mail: nkapur@tuftsmedicalcenter.org. @NavinKapur4.

PERSPECTIVES

COMPETENCY IN MEDICAL KNOWLEDGE: Cardiac fibrosis is a major component of wound healing after MI and serves to reduce ventricular wall stress by replacing cardiomyocyte loss with an organized matrix of collagen. In this study, we identified that BMP-9 plays an important role in regulating cardiac fibrosis after a heart attack. Specifically, we identified that loss of BMP-9 is associated with reduced survival and increased collagen abundance in the LV. Despite increased levels of collagen, loss of BMP-9 also led to a significantly high rate of cardiac rupture, which may be due in part to increased activity of MMP-9 and subsequent collagen degradation. Consistent with this observation, silencing BMP-9 expression in H-CFbs led to increased MMP-9 activity in vitro. These data introduce a novel functional role for BMP-9 in cardiac remodeling and suggest that BMP-9 may be a master regulator of cardiac fibrosis and collagen turnover after MI.

TRANSLATIONAL OUTLOOK: MI remains a major cause of morbidity, mortality, and health care costs. Few studies have explored a functional role for BMPs in cardiac remodeling after MI. This study demonstrates that loss of BMP-9 activity increases mortality and the incidence of cardiac rupture after MI in murine models and further identifies a novel association between BMP-9 expression and BMP-9 activity. These findings suggest that pharmacologic approaches that target the BMP-9 signaling cascade may lead to new treatment modalities for patients experiencing heart attack.

REFERENCES

1. Arena PJ, Mo J, Liu Q, et al. The incidence of acute myocardial infarction after elective spinal fusions or joint replacement surgery in the United States: a large-scale retrospective observational cohort study in 322,585 patients. *Patient Saf Surg*. 2021;15:30. https://doi.org/10.1186/s13037-021-00305-6

2. Ertl G, Frantz S. Healing after myocardial infarction. *Cardiovasc Res*. 2005;66(1):22–32. https://doi.org/10.1016/j.cardiores.2005.01.011

3. Frantz S, Hundertmark MJ, Schulz-Menger J, Bengel FM, Bauersachs J. Left ventricular remodelling post-myocardial infarction: pathophysiology, imaging, and novel therapies. *Eur Heart J*. 2022;43(27):2549–2561.

4. Bujak M, Frangogiannis NG. The role of TGF-beta signaling in myocardial infarction and cardiac remodeling. *Cardiovasc.Res*. 2007;74(2):184–195.

5. Matsui Y, Morimoto J, Uede T. Role of matricellular proteins in cardiac tissue remodeling after myocardial infarction. *World J Biol Chem*. 2010;1(5):69–80.

6. Bujak M, Ren G, Kweon HJ, et al. Essential role of Smad3 in infarct healing and in the pathogenesis of cardiac remodeling. *Circulation*. 2007;116(19):2127–2138.

7. Wooderchak-Donahue WL, McDonald J, O'Fallon B, et al. BMP9 mutations cause a vascular-anomaly syndrome with phenotypic overlap with hereditary hemorrhagic telangiectasia. *Am J Hum Genet*. 2013;93(3):530–537.

8. Gräf S, Haimel M, Bleda M, et al. Identification of rare sequence variation underlying heritable pulmonary arterial hypertension. *Nat Commun*. 2018;9(1):1416. https://doi.org/10.1038/s41467-018-03672-4

9. Nikolic I, Yung LM, Yang P, et al. Bone morphogenetic protein 9 is a mechanistic biomarker of portopulmonary hypertension. *Am J Respir Crit Care Med*. 2019;199(7):891–902.

10. Morine KJ, Qiao X, York S, et al. Bone morphogenetic protein 9 reduces cardiac fibrosis and improves cardiac function in heart failure. *Circulation*. 2018;138(5):513–526.

11. Frangogiannis NG. The extracellular matrix in myocardial injury, repair, and remodeling. *J Clin Invest*. 2017;127(5):1600–1612.

12. Song B, Li WF, Yao Y, et al. BMP9 inhibits the proliferation and migration of fibroblast-like synoviocytes in rheumatoid arthritis via the PI3K/AKT signaling pathway. *Int Immunopharmacol*. 2019;74:105685.

13. Xu J, Zhu D, Sonoda S, et al. Over-expression of BMP4 inhibits experimental choroidal neovascularization by modulating VEGF and MMP-9. *Angiogenesis*. 2012;15(2):213–227.

14. Iyer RP, Jung M, Lindsey ML. MMP-9 signaling in the left ventricle following myocardial infarction. *Am J Physiol Heart Circ Physiol*. 2016;311(1):H190–H198.

15. DeLeon-Pennell KY, Meschiari CA, Jung M, Lindsey ML. Matrix metalloproteinases in myocardial infarction and heart failure. *Prog Mol Biol Transl Sci*. 2017;147:75–100.

16. Qiao X, Bhave S, Swain L, et al. Myocardial injury promotes matrix metalloproteinase-9

activity in the renal cortex in preclinical models of acute myocardial infarction. *J Cardiovasc Transl Res*. 2022;15(2):207–216.

17. Esposito ML, Zhang Y, Qiao X, et al. Left ventricular unloading before reperfusion promotes functional recovery after acute myocardial infarction. *J Am Coll Cardiol*. 2018;72(5):501–514.

18. Monden Y, Kubota T, Tsutsumi T, et al. Soluble TNF receptors prevent apoptosis in infiltrating cells and promote ventricular rupture and remodeling after myocardial infarction. *Cardiovasc Res*. 2007;73(4):794–805.

19. Ma Y, Halade GV, Zhang J, et al. Matrix metalloproteinase-28 deletion exacerbates cardiac dysfunction and rupture after myocardial infarction in mice by inhibiting M2 macrophage activation. *Circ Res*. 2013;112(4):675–688.

20. Hayashidani S, Tsutsui H, Ikeuchi M, et al. Targeted deletion of MMP-2 attenuates early LV rupture and late remodeling after experimental myocardial infarction. *Am J Physiol Heart Circ Physiol*. 2003;285(3):H1229–H1235.

21. Fernández B, Durán AC, Fernández MC, Fernández-Gallego T, Icardo JM, Sans-Coma V. The coronary arteries of the C57BL/6 mouse strains: implications for comparison with mutant models. *J Anat*. 2008;212(1):12–18.

22. Shimazaki M, Nakamura K, Kii I, et al. Periostin is essential for cardiac healing after acute myocardial infarction. *J Exp Med*. 2008;205(2):295–303.

23. Scalise RFM, De Sarro R, Caracciolo A, et al. Fibrosis after myocardial infarction: an overview on cellular processes, molecular pathways, clinical evaluation and prognostic value. *Med Sci*. 2021;9(1):16. https://doi.org/10.3390/medsci9010016

24. Matsumura S, Iwanaga S, Mochizuki S, Okamoto H, Ogawa S, Okada Y. Targeted deletion or pharmacological inhibition of MMP-2 prevents cardiac rupture after myocardial infarction in mice. *J Clin Invest*. 2005;115(3):599–609.

25. Heymans S, Luttun A, Nuyens D, et al. Inhibition of plasminogen activators or matrix metalloproteinases prevents cardiac rupture but impairs therapeutic angiogenesis and causes cardiac failure. *Nat Med*. 1999;5(10):1135–1142.

26. Phatharajaree W, Phrommintikul A, Chattipakorn N. Matrix metalloproteinases and myocardial infarction. *Can J Cardiol*. 2007;23(9):727–733.

27. Wiercinska E, Naber HPH, Pardali E, van der Pluijm G, van Dam H, ten Dijke P. The TGF-β/Smad pathway induces breast cancer cell invasion through the up-regulation of matrix metalloproteinase 2 and 9 in a spheroid invasion model system. *Breast Cancer Res Treat*. 2011;128(3):657–666.

28. Reunanen N, Kähäri V. *Matrix Metalloproteinases in Cancer Cell Invasion*. Landes Bioscience; 2013.

29. Kumagai T, Shimizu T, Takeda K. Bone morphogenetic protein-2 suppresses invasiveness of TSU-Pr1 cells with the inhibition of MMP-9 secretion. *Anticancer Res*. 2006;26(1A):293–298.

30. Wang C, Hu F, Guo S, et al. BMP-6 inhibits MMP-9 expression by regulating heme oxygenase-1 in MCF-7 breast cancer cells. *J Cancer Res Clin Oncol*. 2011;137(6):985–995.

31. Orriols M, Gomez-Puerto MC, ten Dijke P. BMP type II receptor as a therapeutic target in pulmonary arterial hypertension. *Cell Mol Life Sci*. 2017;74(16):2979–2995.

32. Humbert M, McLaughlin V, Gibbs JSR, et al. Sotatercept for the treatment of pulmonary arterial hypertension. *N Engl J Med*. 2021;384(13):1204–1215.

33. Morine KJ, Qiao X, Paruchuri V, et al. Conditional knockout of activin like kinase-1 (ALK-1) leads to heart failure without maladaptive remodeling. *Heart Vessels*. 2017;32(5):628–636.

34. Kim SK, Lee SH, Kim K, Kim BI. ST elevation myocardial infarction in a patient with hereditary hemorrhagic telangiectasia involving the liver. *Korean J Med*. 2017;92(2):182–185.

35. Martínez-Quintana E, Rodríguez-González F, Gopar-Gopar S. Hereditary hemorrhagic telangiectasia and myocardial infarction. *Int J Angiol*. 2016;25(5):e81–e83.

36. Rao S, Khan A, Aiello D. Myocardial infarction in a patient with hereditary hemorrhagic telangiectasia: a case report and review of literature. *Cureus*. 2021;13(5):e15219. https://doi.org/10.7759/cureus.15219

37. Gäddnäs F, Koskela M, Koivukangas V, et al. Markers of collagen synthesis and degradation are increased in serum in severe sepsis: a longitudinal study of 44 patients. *Crit Care*. 2009;13(2):R53. https://doi.org/10.1186/cc7780

38. Quinn KP, Sullivan KE, Liu Z, et al. Optical metrics of the extracellular matrix predict compositional and mechanical changes after myocardial infarction. *Sci Rep*. 2016;6:35823. https://doi.org/10.1038/srep35823

39. Gao X-M, Xu Q, Kiriazis H, Dart AM, Du X-J. Mouse model of post-infarct ventricular rupture: time course, strain- and gender-dependency, tensile strength, and histopathology. *Cardiovasc Res*. 2005;65(2):469–477.

KEY WORDS bone morphogenetic protein-9, fibrosis, matrix metalloproteinase, myocardial infarction

APPENDIX For supplemental figures, please see the online version of this paper.